DESY 94-176

Inclusive Jet Differential Cross Sections in Photoproduction at HERA

ZEUS Collaboration

Abstract

Inclusive jet differential cross sections for the reaction $ep \to jet + X$ at Q^2 below 4 GeV^2 have been measured with the ZEUS detector at HERA using an integrated luminosity of 0.55 pb^{-1}. These cross sections are given in the kinematic region $0.2 < y < 0.85$, for jet pseudorapidities in the ep-laboratory range $-1 < \eta^{jet} < 2$ and refer to jets at the hadron level with a cone radius of one unit in the $\eta - \phi$ plane. These results correspond to quasi-real photoproduction at centre-of-mass energies in the range 130-270 GeV and, approximately, for jet pseudorapidities in the interval $-3 < \eta^{jet}(\gamma p \text{ CMS}) < 0$. These measurements cover a new kinematic regime of the partonic structure of the photon, at typical scales up to ~ 300 GeV^2 and photon fractional momenta down to $x_\gamma \sim 10^{-2}$. Leading logarithm parton shower Monte Carlo calculations, which include both resolved and direct processes and use the predictions of currently available parametrisations of the photon parton distributions, describe in general the shape and magnitude of the measured η^{jet} and E_T^{jet} distributions.

The ZEUS Collaboration

M. Derrick, D. Krakauer, S. Magill, B. Musgrave, J. Repond, J. Schlereth, R. Stanek, R.L. Talaga, J. Thron
Argonne National Laboratory, Argonne, IL, USA [p]

F. Arzarello, R. Ayad[1], G. Bari, M. Basile, L. Bellagamba, D. Boscherini, A. Bruni, G. Bruni, P. Bruni, G. Cara Romeo, G. Castellini[2], M. Chiarini, L. Cifarelli[3], F. Cindolo, F. Ciralli, A. Contin, S. D'Auria, F. Frasconi, I. Gialas, P. Giusti, G. Iacobucci, G. Laurenti, G. Levi, A. Margotti, T. Massam, R. Nania, C. Nemoz, F. Palmonari, A. Polini, G. Sartorelli, R. Timellini, Y. Zamora Garcia[1], A. Zichichi
University and INFN Bologna, Bologna, Italy [f]

A. Bargende, J. Crittenden, K. Desch, B. Diekmann, T. Doeker, M. Eckart, L. Feld, A. Frey, M. Geerts, G. Geitz, M. Grothe, H. Hartmann, D. Haun[4], K. Heinloth, E. Hilger, H.-P. Jakob, U.F. Katz, S.M. Mari, A. Mass, S. Mengel, J. Mollen, E. Paul, Ch. Rembser, R. Schattevoy[4], J.-L. Schneider[4], D. Schramm, J. Stamm, R. Wedemeyer
Physikalisches Institut der Universität Bonn, Bonn, Federal Republic of Germany [c]

S. Campbell-Robson, A. Cassidy, N. Dyce, B. Foster, S. George, R. Gilmore, G.P. Heath, H.F. Heath, T.J. Llewellyn, C.J.S. Morgado, D.J.P. Norman, J.A. O'Mara, R.J. Tapper, S.S. Wilson, R. Yoshida
H.H. Wills Physics Laboratory, University of Bristol, Bristol, U.K. [o]

R.R. Rau
Brookhaven National Laboratory, Upton, L.I., USA [p]

M. Arneodo, L. Iannotti, M. Schioppa, G. Susinno
Calabria University, Physics Dept.and INFN, Cosenza, Italy [f]

A. Bernstein, A. Caldwell, J.A. Parsons, S. Ritz, F. Sciulli, P.B. Straub, L. Wai, S. Yang
Columbia University, Nevis Labs., Irvington on Hudson, N.Y., USA [q]

P. Borzemski, J. Chwastowski, A. Eskreys, K. Piotrzkowski, M. Zachara, L. Zawiejski
Inst. of Nuclear Physics, Cracow, Poland [j]

L. Adamczyk, B. Bednarek, K. Eskreys, K. Jeleń, D. Kisielewska, T. Kowalski, E. Rulikowska-Zarębska, L. Suszycki, J. Zając
Faculty of Physics and Nuclear Techniques, Academy of Mining and Metallurgy, Cracow, Poland [j]

T. Kędzierski, A. Kotański, M. Przybycień
Jagellonian Univ., Dept. of Physics, Cracow, Poland [k]

L.A.T. Bauerdick, U. Behrens, J.K. Bienlein, S. Böttcher[5], C. Coldewey, G. Drews, M. Flasiński[6], D.J. Gilkinson, P. Göttlicher, B. Gutjahr, T. Haas, W. Hain, D. Hasell, H. Heßling, H. Hultschig, Y. Iga, P. Joos, M. Kasemann, R. Klanner, W. Koch, L. Köpke[7], U. Kötz, H. Kowalski, W. Kröger[8], J. Krüger[4], J. Labs, A. Ladage, B. Löhr, M. Löwe, D. Lüke, O. Mańczak, J.S.T. Ng, S. Nickel, D. Notz, K. Ohrenberg, M. Roco, M. Rohde, J. Roldán[9], U. Schneekloth, W. Schulz, F. Selonke, E. Stiliaris[9], T. Voß, D. Westphal, G. Wolf, C. Youngman
Deutsches Elektronen-Synchrotron DESY, Hamburg, Federal Republic of Germany

H.J. Grabosch, A. Leich, A. Meyer, C. Rethfeldt, S. Schlenstedt
DESY-Zeuthen, Inst. für Hochenergiephysik, Zeuthen, Federal Republic of Germany

G. Barbagli, P. Pelfer
University and INFN, Florence, Italy [f]

G. Anzivino, G. Maccarrone, S. De Pasquale, S. Qian, L. Votano
INFN, Laboratori Nazionali di Frascati, Frascati, Italy [f]

A. Bamberger, A. Freidhof, T. Poser[10], S. Söldner-Rembold, J. Schroeder, G. Theisen, T. Trefzger
Fakultät für Physik der Universität Freiburg i.Br., Freiburg i.Br., Federal Republic of Germany [c]

N.H. Brook, P.J. Bussey, A.T. Doyle, I. Fleck, V.A. Jamieson, D.H. Saxon, M.L. Utley, A.S. Wilson
Dept. of Physics and Astronomy, University of Glasgow, Glasgow, U.K. [o]

A. Dannemann, U. Holm, D. Horstmann, H. Kammerlocher[10], B. Krebs[11], T. Neumann, R. Sinkus, K. Wick
Hamburg University, I. Institute of Exp. Physics, Hamburg, Federal Republic of Germany [c]

E. Badura, B.D. Burow, A. Fürtjes[12], L. Hagge, E. Lohrmann, J. Mainusch, J. Milewski, M. Nakahata[13], N. Pavel, G. Poelz, W. Schott, J. Terron[9], F. Zetsche
Hamburg University, II. Institute of Exp. Physics, Hamburg, Federal Republic of Germany [c]

T.C. Bacon, R. Beuselinck, I. Butterworth, E. Gallo, V.L. Harris, B.H. Hung, K.R. Long, D.B. Miller, P.P.O. Morawitz, A. Prinias, J.K. Sedgbeer, A.F. Whitfield
Imperial College London, High Energy Nuclear Physics Group, London, U.K. [o]

U. Mallik, E. McCliment, M.Z. Wang, S.M. Wang, J.T. Wu, Y. Zhang
University of Iowa, Physics and Astronomy Dept., Iowa City, USA [p]

P. Cloth, D. Filges
Forschungszentrum Jülich, Institut für Kernphysik, Jülich, Federal Republic of Germany

S.H. An, S.M. Hong, S.W. Nam, S.K. Park, M.H. Suh, S.H. Yon
Korea University, Seoul, Korea [h]

R. Imlay, S. Kartik, H.-J. Kim, R.R. McNeil, W. Metcalf, V.K. Nadendla
Louisiana State University, Dept. of Physics and Astronomy, Baton Rouge, LA, USA [p]

F. Barreiro[14], G. Cases, R. Graciani, J.M. Hernández, L. Hervás[14], L. Labarga[14], J. del Peso, J. Puga, J.F. de Trocóniz
Univer. Autónoma Madrid, Depto de Física Teóríca, Madrid, Spain [n]

F. Ikraiam, J.K. Mayer[15], G.R. Smith
University of Manitoba, Dept. of Physics, Winnipeg, Manitoba, Canada [a]

F. Corriveau, D.S. Hanna, J. Hartmann, L.W. Hung, J.N. Lim, C.G. Matthews, P.M. Patel, L.E. Sinclair, D.G. Stairs, M. St.Laurent, R. Ullmann, G. Zacek
McGill University, Dept. of Physics, Montreal, Quebec, Canada [a, b]

V. Bashkirov, B.A. Dolgoshein, A. Stifutkin
Moscow Engineering Physics Institute, Mosocw, Russia [l]

G.L. Bashindzhagyan, P.F. Ermolov, L.K. Gladilin, Y.A. Golubkov, V.D. Kobrin, V.A. Kuzmin, A.S. Proskuryakov, A.A. Savin, L.M. Shcheglova, A.N. Solomin, N.P. Zotov
Moscow State University, Institute of Nuclear Pysics, Moscow, Russia [m]

S. Bentvelsen, M. Botje, F. Chlebana, A. Dake, J. Engelen, P. de Jong[16], M. de Kamps, P. Kooijman, A. Kruse, V. O'Dell[17], A. Tenner, H. Tiecke, W. Verkerke, M. Vreeswijk, L. Wiggers, E. de Wolf, R. van Woudenberg
NIKHEF and University of Amsterdam, Netherlands [i]

D. Acosta, B. Bylsma, L.S. Durkin, K. Honscheid, C. Li, T.Y. Ling, K.W. McLean, W.N. Murray, I.H. Park, T.A. Romanowski[18], R. Seidlein
Ohio State University, Physics Department, Columbus, Ohio, USA [p]

D.S. Bailey, G.A. Blair[19], A. Byrne, R.J. Cashmore, A.M. Cooper-Sarkar, D. Daniels[20], R.C.E. Devenish, N. Harnew, M. Lancaster, P.E. Luffman[21], L. Lindemann, J. McFall, C. Nath, A. Quadt, H. Uijterwaal, R. Walczak, F.F. Wilson, T. Yip
Department of Physics, University of Oxford, Oxford, U.K. [o]

G. Abbiendi, A. Bertolin, R. Brugnera, R. Carlin, F. Dal Corso, M. De Giorgi, U. Dosselli, S. Limentani, M. Morandin, M. Posocco, L. Stanco, R. Stroili, C. Voci
Dipartimento di Fisica dell' Universita and INFN, Padova, Italy [f]

J. Bulmahn, J.M. Butterworth, R.G. Feild, B.Y. Oh, J.J. Whitmore[22]
Pennsylvania State University, Dept. of Physics, University Park, PA, USA [q]

G. D'Agostini, M. Iori, G. Marini, M. Mattioli, A. Nigro, E. Tassi
Dipartimento di Fisica, Univ. 'La Sapienza' and INFN, Rome, Italy [f]

J.C. Hart, N.A. McCubbin, K. Prytz, T.P. Shah, T.L. Short
Rutherford Appleton Laboratory, Chilton, Didcot, Oxon, U.K. [o]

E. Barberis, N. Cartiglia, T. Dubbs, C. Heusch, M. Van Hook, B. Hubbard, W. Lockman,
J.T. Rahn, H.F.-W. Sadrozinski, A. Seiden
University of California, Santa Cruz, CA, USA [p]

J. Biltzinger, R.J. Seifert, A.H. Walenta, G. Zech
Fachbereich Physik der Universität-Gesamthochschule Siegen, Federal Republic of Germany [c]

H. Abramowicz, G. Briskin, S. Dagan[23], A. Levy[23]
School of Physics, Tel-Aviv University, Tel Aviv, Israel [e]

T. Hasegawa, M. Hazumi, T. Ishii, M. Kuze, S. Mine, Y. Nagasawa, T. Nagira, M. Nakao, I. Suzuki, K. Tokushuku,
S. Yamada, Y. Yamazaki
Institute for Nuclear Study, University of Tokyo, Tokyo, Japan [g]

M. Chiba, R. Hamatsu, T. Hirose, K. Homma, S. Kitamura, S. Nagayama, Y. Nakamitsu
Tokyo Metropolitan University, Dept. of Physics, Tokyo, Japan [g]

R. Cirio, M. Costa, M.I. Ferrero, L. Lamberti, S. Maselli, C. Peroni, R. Sacchi, A. Solano, A. Staiano
Universita di Torino, Dipartimento di Fisica Sperimentale and INFN, Torino, Italy [f]

M. Dardo
II Faculty of Sciences, Torino University and INFN - Alessandria, Italy [f]

D.C. Bailey, D. Bandyopadhyay, F. Benard, M. Brkic, M.B. Crombie, D.M. Gingrich[24], G.F. Hartner, K.K. Joo,
G.M. Levman, J.F. Martin, R.S. Orr, C.R. Sampson, R.J. Teuscher
University of Toronto, Dept. of Physics, Toronto, Ont., Canada [a]

C.D. Catterall, T.W. Jones, P.B. Kaziewicz, J.B. Lane, R.L. Saunders, J. Shulman
University College London, Physics and Astronomy Dept., London, U.K. [o]

K. Blankenship, J. Kochocki, B. Lu, L.W. Mo
Virginia Polytechnic Inst. and State University, Physics Dept., Blacksburg, VA, USA [q]

W. Bogusz, K. Charchuła, J. Ciborowski, J. Gajewski, G. Grzelak, M. Kasprzak, M. Krzyżanowski,
K. Muchorowski, R.J. Nowak, J.M. Pawlak, T. Tymieniecka, A.K. Wróblewski, J.A. Zakrzewski, A.F. Żarnecki
Warsaw University, Institute of Experimental Physics, Warsaw, Poland [j]

M. Adamus
Institute for Nuclear Studies, Warsaw, Poland [j]

Y. Eisenberg[23], C. Glasman, U. Karshon[23], D. Revel[23], A. Shapira
Weizmann Institute, Nuclear Physics Dept., Rehovot, Israel [d]

I. Ali, B. Behrens, S. Dasu, C. Fordham, C. Foudas, A. Goussiou, R.J. Loveless, D.D. Reeder,
S. Silverstein, W.H. Smith
University of Wisconsin, Dept. of Physics, Madison, WI, USA [p]

T. Tsurugai
Meiji Gakuin University, Faculty of General Education, Yokohama, Japan

S. Bhadra[25], W.R. Frisken, K.M. Furutani
York University, Dept. of Physics, North York, Ont., Canada [a]

[1] supported by Worldlab, Lausanne, Switzerland
[2] also at IROE Florence, Italy
[3] now at Univ. of Pisa, Italy
[4] now a self-employed consultant
[5] now at Tel Aviv Univ., Faculty of Engineering
[6] now at Inst. of Computer Science, Jagellonian Univ., Cracow
[7] now at Univ. of Mainz
[8] now at Univ. of California, Santa Cruz
[9] supported by the European Community
[10] now at DESY
[11] now with Herfurth GmbH, Hamburg
[12] now at CERN
[13] now at Institute for Cosmic Ray Research, University of Tokyo
[14] on leave of absence at DESY, supported by DGICYT
[15] now at Univ. of Toronto
[16] now at MIT, Cambridge, MA
[17] now at Fermilab., Batavia, IL
[18] now at Department of Energy, Washington
[19] now at RHBNC, Univ. of London, England
[20] Fulbright Scholar 1993-1994
[21] now at Cambridge Consultants, Cambridge, U.K.
[22] on leave and partially supported by DESY 1993-95
[23] supported by a MINERVA Fellowship
[24] now at Centre for Subatomic Research, Univ.of Alberta, Canada and TRIUMF, Vancouver, Canada
[25] now at DESY

[a] supported by the Natural Sciences and Engineering Research Council of Canada
[b] supported by the FCAR of Quebec, Canada
[c] supported by the German Federal Ministry for Research and Technology (BMFT)
[d] supported by the MINERVA Gesellschaft für Forschung GmbH, and by the Israel Academy of Science
[e] supported by the German Israeli Foundation, and by the Israel Academy of Science
[f] supported by the Italian National Institute for Nuclear Physics (INFN)
[g] supported by the Japanese Ministry of Education, Science and Culture (the Monbusho) and its grants for Scientific Research
[h] supported by the Korean Ministry of Education and Korea Science and Engineering Foundation
[i] supported by the Netherlands Foundation for Research on Matter (FOM)
[j] supported by the Polish State Committee for Scientific Research (grant No. 204209101)
[k] supported by the Polish State Committee for Scientific Research (grant No. PB 861/2/91 and No. 2 2372 9102, grant No. PB 2 2376 9102 and No. PB 2 0092 9101)
[l] partially supported by the German Federal Ministry for Research and Technology (BMFT)
[m] supported by the German Federal Ministry for Research and Technology (BMFT), the Volkswagen Foundation, and the Deutsche Forschungsgemeinschaft
[n] supported by the Spanish Ministry of Education and Science through funds provided by CICYT
[o] supported by the Particle Physics and Astronomy Research Council
[p] supported by the US Department of Energy
[q] supported by the US National Science Foundation

1 Introduction

In photon-proton reactions, two types of QCD processes contribute to jet production at leading order [1, 2]: either the photon interacts directly with a parton in the proton (the direct process) or the photon acts as a source of partons which scatter off those in the proton (the resolved process). The final state consists of two partons from the hard process, carrying large transverse momenta and balancing each other, with the proton remnant carrying little transverse momentum. In resolved processes, a hadronic system from the fragmentation of the spectator parton(s) in the photon is also expected.

At HERA, photoproduction is studied via ep scattering at low four-momentum transfers ($Q^2 \approx 0$, in what follows referred to as low Q^2 interactions). The first year of HERA operation led to the observation of hard scattering in γp collisions with evidence for multijet structure and the presence of the resolved process [3, 4]. The study of two-jet events allowed the separation of the resolved and direct processes [5].

Differential jet cross sections as a function of transverse energy ($d\sigma/dE_T^{jet}$) and pseudorapidity ($d\sigma/d\eta^{jet}$) in the low Q^2 regime are sensitive to the partonic content of the proton and the photon [2, 6]. The dependence on the parton content of the photon can be isolated by studying jet production at sufficiently high E_T^{jet}. In this region, jet cross sections involve proton parton distributions in a kinematic range constrained by previous experiments. Before HERA, the hadronic structure of the photon has been experimentally investigated mainly in inclusive $e\gamma$ deep inelastic scattering at e^+e^- colliders [7]. Leading order (LO) [8, 9] and next-to-leading order (NLO) [10, 11, 12] fits to these data allowed the extraction of the quark densities in the photon but left the gluon density essentially unconstrained. Recently, measurements of jet cross sections in $\gamma\gamma$ interactions at TRISTAN have been presented [13]. These jet cross sections probed the photon structure at scales $\hat{Q}_\gamma^2 \sim 6 - 100$ GeV^2, where $\hat{Q}_\gamma^2$ is taken to be the squared transverse momenta of the outgoing partons, and involved partons in the photon with fractional momenta (x_γ) down to $\sim 10^{-1}$. The comparison to LO QCD predictions showed that the contribution from the gluon content of the photon was essential to describe these measurements successfully. The measurement of $d\sigma/dE_T^{jet}$ and $d\sigma/d\eta^{jet}$ for inclusive jet production at low Q^2 at HERA tests the predictions of the parametrisations of the photon parton distributions at higher $\hat{Q}_\gamma^2$ scales and gives information concerning the gluon density at lower x_γ values with respect to existing results. First measurements of $d\sigma/d\eta^{jet}$ by the H1 Collaboration [14], in a narrower kinematic range than reported in the present paper, indicated a discrepancy with respect to LO QCD expectations.

In this paper we extend the measurement of $d\sigma/dE_T^{jet}$ and $d\sigma/d\eta^{jet}$ to a wider region of E_T^{jet} (8 GeV $< E_T^{jet} <$ 41 GeV) and η^{jet} ($-1 < \eta^{jet} < 2$) with respect to existing results. This kinematic region corresponds to photoproduction interactions at centre-of-mass energies in the range 130-270 GeV. The η^{jet} range studied in the ep laboratory frame corresponds to different angular ranges in the γp centre-of-mass system (CMS) depending on the longitudinal boost. For the bulk of the data it is approximately $-3 < \eta^{jet}(\mathrm{CMS}) < 0$. These measurements probe $\hat{Q}_\gamma^2$ scales up to ~ 300 GeV^2 and x_γ down to $\sim 10^{-2}$. LO QCD calculations including both resolved and direct processes are compared to the measured jet cross sections in this new kinematic regime. The data sample used in this analysis was collected during 1993 with the ZEUS detector at HERA and corresponds to an integrated luminosity of 0.55 pb^{-1}.

2 Experimental setup

2.1 HERA operation

The experiment was performed at the electron-proton collider HERA using the ZEUS detector. During 1993 HERA operated with electrons of energy $E_e = 26.7$ GeV colliding with protons of energy $E_p = 820$ GeV. HERA is designed to run with 210 bunches separated by 96 ns in each of the electron and proton rings. For the 1993 data taking, 84 paired bunches were filled for each beam, and, in addition, 10 electron and 6 proton bunches were left unpaired for background studies. The electron and proton beam currents were typically 10 mA and typical instantaneous luminosities were $\approx 6 \cdot 10^{29}$ cm^{-2} s^{-1}.

2.2 The ZEUS detector and trigger conditions

ZEUS is a multipurpose magnetic detector whose configuration for the 1993 running period has been described elsewhere [15, 16]. Here we give a brief description concentrating on those parts of the detector relevant for the present analysis.

Charged particles are tracked by two concentric cylindrical drift chambers, the vertex detector (VXD) and the central tracking detector (CTD), which operate in a magnetic field of 1.43 T provided by a thin superconducting coil. The coil is surrounded by a high-resolution uranium-scintillator calorimeter (CAL) divided into three parts, forward[1] (FCAL) covering the pseudorapidity[2] region $4.3 \geq \eta_d \geq 1.1$, barrel (BCAL) covering the central region $1.1 \geq \eta_d \geq -0.75$ and rear (RCAL) covering the backward region $-0.75 \geq \eta_d \geq -3.8$. The solid angle coverage is 99.7% of 4π. The CAL parts are subdivided into towers which in turn are subdivided longitudinally into electromagnetic (EMC) and hadronic (HAC) sections. The sections are subdivided into cells, each of which is viewed by two photomultiplier tubes. The CAL is compensating, giving equal response to hadrons and electrons. Measurements under test beam conditions show that the energy resolution is $\sigma_E/E = 0.18/\sqrt{E}$ (E in GeV) for electrons and $\sigma_E/E = 0.35/\sqrt{E}$ for hadrons [17]. In the analysis presented here CAL cells with EMC (HAC) energy below 60 MeV (110 MeV) are excluded to minimize the effect of calorimeter noise. This noise is dominated by uranium activity and has an r.m.s. value below 19 MeV for EMC cells and below 30 MeV for HAC cells. For measuring the luminosity as well as for tagging very small Q^2 processes, we use two lead-scintillator calorimeters located at 107 m and 35 m downstream from the interaction point in the electron direction [18]. They detect the bremsstrahlung photons and the scattered electrons respectively.

Data were collected using a three level trigger [15]. The First Level Trigger (FLT) is built as a deadtime-free pipeline. The FLT for the sample of events analysed in this paper required a logical OR of different conditions on sums of energy in the CAL cells. The average FLT acceptance for the events under study was $\approx 90\%$. The Second Level Trigger used information from a subset of detector components to differentiate physics events from backgrounds consisting mostly of proton beam gas interactions. The Third Level Trigger applies physics specific selections using the full event information. For this analysis the following conditions were required: a) the event has a reconstructed vertex from the tracking chambers (VXD+CTD) with the z

[1] The ZEUS coordinate system is defined as right-handed with the z axis pointing in the proton beam direction, hereafter referred to as forward, and the x axis horizontal, pointing towards the centre of HERA.

[2] The pseudorapidity is defined as $-\ln(\tan\frac{\theta}{2})$, where the polar angle θ is taken with respect to the proton beam direction, and is denoted by η_d (η) when the polar angle is taken with respect to the nominal interaction point (the reconstructed vertex of the interaction).

value in the range $|z| < 75$ cm; b) $E - p_z \geq 8$ GeV, where E is the total energy as measured by the CAL and p_z is the z-component of the vector $\vec{p} = \Sigma_i E_i \vec{r}_i$ (E_i is the energy of the cell i, and $\vec{r}_i$ is a unit vector along the line joining the reconstructed vertex and the geometric centre of the cell i; the sum runs over all cells); c) $p_z/E \leq 0.94$ to reject beam-gas interactions; and d) the total transverse energy as measured by the CAL, excluding the cells whose polar angles are below 10°, exceeds 12 GeV.

3 Data selection criteria

In order to select ep interactions with jet activity, a search for jet structure using the CAL cells (see section 5) is performed, and events with at least one jet fulfilling the conditions $E_{T,cal}^{jet} > 6$ GeV and $-1 < \eta_{cal}^{jet} < 2$ are retained. A total of 30,366 events satisfy these conditions. The contamination from beam-gas interactions, cosmic showers and halo muons is negligible after demanding: a) at least two tracks pointing to the vertex; b) if there are only two tracks pointing to the vertex the opening angle between them (α) satisfy $\cos\alpha > -0.996$; c) the vertex position along the beam axis lies in the range -48 cm $< z < 36$ cm; d) less than five tracks not associated with the vertex and compatible with an interaction upstream in the direction of the proton beam; and e) the total missing transverse momentum ($\not{p}_T$) be small compared to the total transverse energy (E_T^{tot}) by requiring $\not{p}_T/\sqrt{E_T^{tot}} < 2$ GeV$^{\frac{1}{2}}$. The last condition also rejects events from ep deep inelastic scattering (DIS) charged current interactions where the final state neutrino remains undetected. DIS neutral current events are removed from the sample as described in our previous publications [4, 5].

At this stage the sample consists of events from ep interactions with $Q^2 < 4$ GeV^2. The γp centre-of-mass energy (W) is calculated using the expression $W = \sqrt{4yE_eE_p}$, where y is the inelasticity variable. The event sample is restricted to the kinematic range $0.2 < y < 0.85$ using the following procedure. The method of Jacquet-Blondel [19], applied to the low Q^2 regime [20], $y_{JB} = (E - p_z)/(2E_e)$, is used to estimate y from the energies measured in the CAL cells. For events tagged by an electron in the electron calorimeter of the luminosity monitor, the variable y is measured independently using the relation $y_e = 1 - E_e'(1 - \cos\theta_e')/(2E_e)$, where E_e' and θ_e' are the energy and the angle of the scattered electron, respectively. A comparison of y_e and y_{JB} shows that y_{JB} is systematically smaller by approximately 20%. This discrepancy is attributed to the energy lost in the inactive material in front of the CAL and to particles lost in the rear beam pipe. It is adequately reproduced in the Monte Carlo simulation of the detector. To allow for this effect, in the event selection we required $0.16 < y_{JB} < 0.7$.

The final sample consists of 19,485 events containing 24,504 jets. A fraction of these events is expected to have an electron observed in the electron calorimeter of the luminosity monitor, whose acceptance reaches up to $Q^2 \approx 0.02$ GeV^2 [21]. In fact, 5,065 of the 19,485 events are found with such electrons, which when combined with the acceptance, indicates that the bulk of the data originate from the photoproduction regime ($Q^2 \approx 0$). The only significant background is from unidentified DIS neutral current interactions with $Q^2 > 4$ GeV^2, which is estimated to be below 2% using Monte Carlo techniques.

4 Monte Carlo simulation

Samples of events were generated using Monte Carlo simulations to determine the response of the detector to jets of hadrons. From this, the correction factors for the inclusive jet cross

sections were obtained.

The programs PYTHIA-5.6 [22] and HERWIG-5.7 [23] were used to generate photoproduction events via resolved and direct processes. The lepton-photon vertex was modelled according to the Weizsäcker-Williams approximation in PYTHIA. In the case of HERWIG, the exact matrix elements were used for direct processes ($eg \to eq\bar{q}$ and $eq \to eqg$) and the equivalent photon approximation for resolved processes. The effects of initial state bremsstrahlung from the electron were simulated by PYTHIA using the NLO electron structure function [24]. However, radiative corrections in our kinematic region, where W is larger than 100 GeV, are expected to be negligible [21]. Events were generated using the leading order predictions by GRV [10] for the photon parton distributions and MRSD_ [25] for the proton parton distributions. In addition, samples of events using the LAC1 parametrisation [9] for the photon and MRSD_0 [25] for the proton parton distributions were studied. In these generators, the partonic processes were simulated using leading order matrix elements, with the inclusion of initial and final state parton showers. Fragmentation into hadrons was performed using the LUND [26] string model as implemented in JETSET [27] in the case of PYTHIA, and the cluster model in the case of HERWIG. Samples of events were generated with different values of the cutoff on the transverse momentum of the two outgoing partons starting at $\hat{p}_{Tmin} = 2.5$ GeV/c.

In addition, Monte Carlo events from low Q^2 diffractive processes were generated. It is expected that these processes contribute to inclusive jet production [28], and experimental evidence for their existence has been found at HERA by the H1 and ZEUS Collaborations [29]. The final states corresponding to these processes, which are not accounted for by either PYTHIA or HERWIG, have been simulated using the program POMPYT [30]. The Monte Carlo events were generated with the cutoff on the transverse momentum set to $\hat{p}_{Tmin} = 3$ GeV/c in the two-body hard collision.

All generated events were passed through the ZEUS detector and trigger simulation programs [15]. They were reconstructed using standard ZEUS off-line programs and passed through the same analysis chain as the data.

5 Jet search

A cone algorithm in pseudorapidity (η) - azimuth (ϕ) space [31, 32] is used to reconstruct jets, from the energy depositions in the CAL cells in both data and generated events, and also from the final state hadrons in the generated events.

The procedure is explained in detail for the jet reconstruction from the CAL energies (*cal* jets). CAL cells satisfying the thresholds explained in section 2.2 are considered with their $\eta - \phi$ determined from the unit vectors joining the vertex of the interaction and the geometric centres of the cells. In the first step, each CAL cell with a transverse energy in excess of 300 MeV is considered as a seed for the search. These seeds are combined if their distance in $\eta - \phi$ space, $R = \sqrt{\Delta\phi^2 + \Delta\eta^2}$, is smaller than 1 unit. Then a cone of radius $R = 1$ is drawn around each seed and the CAL cells within that cone are combined to form a cluster. The axis of the cluster is defined according to the Snowmass convention [32]: $\eta^{cluster}$ ($\phi^{cluster}$) is the transverse energy weighted mean pseudorapidity (azimuth) of all the CAL cells belonging to that cluster. A new cone of radius 1 unit is then drawn around the axis of the cluster. All cells inside the cone are used to recalculate a new cluster axis. The procedure is iterated until the content of the cluster does not change.

The energy sharing of overlapping clusters is then considered. Two clusters are merged if the common transverse energy exceeds 75% of the total transverse energy of the cluster with

the lowest transverse energy; otherwise two different clusters are formed and the common cells are assigned to the nearest cluster. Finally a cluster is called a jet if $E_T^{cluster}$ exceeds 6 GeV. In the present analysis only jets with η^{jet} in the range $-1 < \eta^{jet} < 2$ are selected.

In the case of Monte Carlo events, the same jet algorithm is also applied to the final state particles. The jets found are called *had* jets. In this search, all particles with lifetimes larger than 10^{-13} s and with polar angles between 5° and 175° are considered. The variables associated with the *had* jets are denoted by $E_{T,had}^{jet}$, η_{had}^{jet}, and ϕ_{had}^{jet}, while the ones for the *cal* jets by $E_{T,cal}^{jet}$, η_{cal}^{jet}, and ϕ_{cal}^{jet}.

The characteristics of the *cal* jets in the Monte Carlo samples of PYTHIA and HERWIG were compared to those in the data. As the energy corrections to the *cal* jets and the correction factors to the observed inclusive jet distributions depend on the features of the *had* jets, the characteristics of the jets in the data must be adequately reproduced by the Monte Carlo simulations. Two studies have been performed. The first one investigates the charged particle content of the jets in the region where tracks are well reconstructed ($|\eta_{cal}^{jet}| < 1$). The second check extends the study to both charged and neutral particles in the entire η_{cal}^{jet} region under consideration ($-1 < \eta_{cal}^{jet} < 2$).

In the $|\eta_{cal}^{jet}| < 1$ region, the multiplicity distribution and the p_T-spectrum of charged particles within the *cal* jets have been compared for data and Monte Carlo samples using tracks reconstructed by the CTD+VXD. The tracks were required to be in the ranges $|\eta^{track}| < 1.5$ and $p_T^{track} > 300$ MeV, where p_T^{track} is the transverse momentum of the track with respect to the beam axis. Tracks were associated with a *cal* jet when the extrapolated trajectory reached the CAL within the cone of the *cal* jet. PYTHIA describes all the measured distributions well, while HERWIG underestimates the multiplicity by $\approx 11\%$ and exhibits a p_T^{track}-spectrum which is somewhat too hard.

The second study is extended to both charged and neutral particles by investigating the transverse energy profile around the jet in $\Delta\eta \equiv \eta_{cell} - \eta_{cal}^{jet}$ and $\Delta\phi \equiv \phi_{cell} - \phi_{cal}^{jet}$. The density of transverse energy in the hemisphere of the jet (integrated over $|\Delta\phi| < \pi/2$), per unit of pseudorapidity, as a function of $\Delta\eta$, is shown in Figure 1 (top row) for the inclusive jet data sample (black dots) in three η_{cal}^{jet} ranges: $-1 < \eta_{cal}^{jet} < 0$, $0 < \eta_{cal}^{jet} < 1$ and $1 < \eta_{cal}^{jet} < 2$. In addition, the density of transverse energy integrated over $|\Delta\eta| < 1$, as a function of $\Delta\phi$, is presented in the bottom row of Figure 1 for the same sample. The Monte Carlo expectations from the event sample of PYTHIA including the resolved plus direct contributions (histogram) are compared to the data in the same figure: the two contributions are added according to the cross sections given by the generators. Here the comparison between data and Monte Carlo expectations has been made in terms of CAL transverse energy densities uncorrected for detector effects. The transverse energy profile within the jet and its vicinity for the data is well described by the Monte Carlo expectations in most of the η_{cal}^{jet} range considered. The exact height of the peak in the Monte Carlo distributions has been studied and observed to depend on the particular admixture of resolved and direct processes used. The distribution outside the peak hardly changes except when the extreme choice of including only direct processes is considered. The decrease of the $\Delta\eta$ distribution seen both in data and Monte Carlo expectations in the region $\Delta\eta > 2$ for the forward jets ($1 < \eta_{cal}^{jet} < 2$) is a geometric effect: the most forward edge of the FCAL is at $\eta_d = 4.3$. These comparisons indicate that, although there is some discrepancy for the forward-going jets in the region $\Delta\eta > 1$, the core of the jet (i.e. $|\Delta\eta| < 1$ and $|\Delta\phi| < \pi/2$) is adequately reproduced by PYTHIA.

The results of these studies show that the Monte Carlo simulations adequately reproduce the properties of the jets. Therefore, the Monte Carlo simulations have been used to determine

the energy corrections and correction factors for jets in the region $-1 < \eta^{jet}_{cal} < 2$.

5.1 Energy corrections to jets

The comparison of the reconstructed variables of the *had* jets and the *cal* jets was made using the Monte Carlo samples. The matching between the *cal* and *had* jets was based on the distance in the $\eta - \phi$ plane. The pair of *had-cal* jets closest in $R = \sqrt{\Delta\eta^2 + \Delta\phi^2}$ with $R < 1$ was considered to be matched. Unmatched *cal* jets were counted as impurity and unmatched *had* jets as inefficiency. The appropriate corrections are discussed in the next section. From the comparison of the reconstructed jet variables it is concluded that no significant systematic shift in the angular variable η^{jet}_{cal} (ϕ^{jet}_{cal}) with respect to η^{jet}_{had} (ϕ^{jet}_{had}) is present, and that the resolution in η^{jet}_{cal} is 0.07 units of pseudorapidity and in ϕ^{jet}_{cal} is 5°. On the other hand, the transverse energy of the *cal* jet underestimates that of the *had* jets by an average amount of $\approx 16\%$ with a spread of 11%.

The Monte Carlo samples were used to determine the transverse energy corrections to *cal* jets averaged over the azimuthal angle of the jet. These corrections have been constructed as multiplicative factors, $C(E^{jet}_{T,cal}, \eta^{jet}_{cal})$, which, when applied to the E_T of the *cal* jets give the 'corrected' transverse energies of the jets, $E^{jet}_T = C(E^{jet}_{T,cal}, \eta^{jet}_{cal}) \times E^{jet}_{T,cal}$. As was mentioned above, no correction is needed for η^{jet} ($\eta^{jet} \approx \eta^{jet}_{cal}$).

The transverse energy correction computed with the event samples of PYTHIA for values above 10 GeV is approximately flat as a function of $E^{jet}_{T,cal}$ and varies between 1.08 and 1.18 depending on η^{jet}_{cal}. For $E^{jet}_{T,cal}$ near threshold, $E^{jet}_{T,cal} \approx 6$ GeV, this correction procedure can give values as large as 1.40. Separate transverse energy corrections were also obtained using the event samples of HERWIG. They are expected to be slightly different from the corrections determined using the PYTHIA samples because the energy losses and, consequently, the corrections, depend on the multiplicity and transverse momentum spectrum of the individual hadrons forming the jets. These features depend on the specific fragmentation scheme used and on the flavour content of the final state partons produced by the generator. The consistency between the various corrections has been checked by applying the corrections obtained with a given generator to a sample of events from another generator. On the average, the transverse energy of the *had* jet is recovered to better than $\pm$ 5%.

The correctness of the simulation of those aspects of the detector which affect the energy losses in the jets was checked by the following procedure. In the central region, $|\eta^{jet}_{cal}| < 1$, the momenta of the tracks in the *cal* jet were used to determine the total transverse energy carried by the charged particles, $E^{jet}_{T,tracks}$. Then, the ratio $E^{jet}_{T,tracks}/E^{jet}_{T,cal}$ was formed, and the distributions of this ratio in the inclusive *cal* jet sample in data and Monte Carlo simulations were compared. From this comparison it was concluded that the energy scale of the jets with $|\eta^{jet}| < 1$ is correct to within $\pm$ 5%. In the forward region, $1 < \eta^{jet} < 2$, the energy scale of the jets was studied using the transverse energy imbalance in dijet events with one jet in the central region and the other in the forward region. The comparison of the distributions of the ratio $E^{jet}_{T,cal}$(forward jet)/$E^{jet}_{T,cal}$(central jet) in data and Monte Carlo samples showed that in the forward region the energy scale of the jets is also correct to within $\pm$ 5%.

5.2 Acceptance corrections to inclusive jet distributions

The samples of Monte Carlo generated events of resolved and direct processes were used to compute the acceptance corrections to the inclusive jet distributions. These correction factors

take into account the efficiency of the trigger, the selection criteria and the purity and efficiency of the jet reconstruction. In particular, these factors correct for the migration in the variable y_{JB} and yield cross sections for the true kinematic range $0.2 < y < 0.85$. After the jet transverse energy corrections, the purity is $\approx 60\%$ for jets at threshold and increases rapidly as E_T^{jet} increases, being greater than 90% for $E_T^{jet} > 17$ GeV. The efficiency is $\approx 60\%$ for jets at threshold and is larger than 80% for $E_T^{jet} > 11$ GeV. The differential cross sections are then obtained by applying bin-by-bin corrections to the inclusive jet distributions of the data sample in the variables E_T^{jet} and η^{jet}. For this approach to be valid, the uncorrected inclusive jet distributions in the data must be described by the Monte Carlo simulations. The predictions of the generators PYTHIA and HERWIG for the distributions before correction for acceptance were compared to the data for several choices of the parton densities in the photon and proton and for various combinations of the processes involved. A good description of the E_T^{jet} and η^{jet} data distributions by the Monte Carlo simulations is obtained only when the contributions of both direct and resolved processes are included.

The acceptance correction factors for the inclusive jet cross section $d\sigma/d\eta^{jet}$ ($d\sigma/dE_T^{jet}$) vary between 0.90 and 1.17 (0.96 and 1.37) using the event samples of PYTHIA with resolved and direct processes. The dependence of these correction factors on the choice of parametrisations of the parton densities in the photon and proton, fragmentation scheme and type of process was studied and found to be small. The resulting differences are taken into account as contributions to the total systematic uncertainty assigned to the measurements reported in the next section. In addition, the dependence on the environment in which the jets are embedded was studied by using the events generated with the program POMPYT. The POMPYT program simulates final states without colour flow between the partons that undergo the hard scatter and the spectator partons in the proton. Additional parton radiation is suppressed due to the low centre-of-mass energy available in the parton-parton collision system. Thus the jet environment is very different in non-diffractive events simulated by PYTHIA (or HERWIG) and diffractive events simulated by POMPYT. The correction factors varied by less than 10%, showing that they depend very weakly on the jet environment.

6 Inclusive jet cross sections

Using the selected data sample of jets and the correction procedures described above, differential jet cross sections in the kinematic region defined by $Q^2 \leq 4$ GeV^2 and $0.2 < y < 0.85$ have been measured. These cross sections, $d\sigma/d\eta^{jet}$ and $d\sigma/dE_T^{jet}$, refer to jets at the hadron level with a cone radius of one unit in $\eta - \phi$ space. We note that these cross sections are for the reaction $ep \rightarrow jet + X$. The cross section $d\sigma/d\eta^{jet}$ has been measured in the η^{jet} range between -1 and 2 integrated over E_T^{jet} from three different thresholds ($E_T^{jet} > 8$, 11 and 17 GeV). The cross section $d\sigma/dE_T^{jet}$ has been measured in the E_T^{jet} range above 8 GeV integrated over two different η^{jet} ranges ($-1 < \eta^{jet} < 2$ and $-1 < \eta^{jet} < 1$).

The results for $d\sigma/d\eta^{jet}$ and $d\sigma/dE_T^{jet}$ are presented in Figures 2 to 4. The statistical and systematic uncertainties are also shown. A detailed study of the sources contributing to the systematic uncertainties of the measurements was carried out [33, 34]. They were classified into six groups (an average value of the systematic uncertainty for each item is indicated in parentheses):

- Choice of the parton densities in the proton (MRSD$_-$ and MRSD$_0$) and photon (GRV and LAC1) for the generation of the PYTHIA Monte Carlo samples ($\approx 0.2\%$ for the proton

and $\approx 3\%$ for the photon).

- Simulation of either resolved or resolved plus direct processes in the generation of the multihadronic final states by PYTHIA ($\approx 3\%$).
- Inclusion of a contribution from hard diffraction processes simulated by POMPYT[3] to the non-diffractive event samples of PYTHIA ($\approx 0.5\%$).
- Use of the HERWIG generator to evaluate the energy corrections to *cal* jets and the correction factors to the observed inclusive jet distributions ($\approx 7\%$).
- Variation of the absolute energy scale of the *cal* jets by $\pm$ 5% to take into account the uncertainty of the present description of the inactive material in front of the CAL ($\approx 20\%$).
- Uncertainties in the simulation of the trigger and variation of the cuts used to select the data within the ranges allowed by the comparison between data and Monte Carlo simulations ($\approx 5\%$).

The dominant source of systematic error is the uncertainty in the absolute energy scale of the *cal* jets. The statistical errors on the measurements are indicated as thick error bars in Figures 2 to 4. The systematic uncertainties not associated with the energy scale of the jets have been added in quadrature to the statistical errors and are shown as thin error bars. The additional uncertainty due to the energy scale of the jets is shown as a shaded band. We note that the systematic uncertainties have a large degree of correlation from bin to bin. These systematic uncertainties are to be understood as the maximum possible error associated with each data point. In addition, there is an overall normalisation uncertainty of 3.3% from the luminosity determination, which is not included.

The measured differential cross sections are compared to the absolute predictions of the PYTHIA generator including resolved plus direct processes with a cutoff $\hat{p}_{Tmin} = 5$ GeV/c. They have been obtained by selecting *had* jets using the same jet algorithm as for the data. The Monte Carlo calculations using MRSD_ [25] for the proton and one of LAC1 [9], GRV-HO [10], GS-HO [11] or ACFGP-HO(mc) [12] for the photon parton distributions are compared to our measurements in Figures 2 to 4. The parton distributions in the proton and the photon are evaluated at the hard scale set by the transverse momentum of the two outgoing partons, $\hat{Q}_p^2 = \hat{Q}_\gamma^2 = \hat{p}_T^2$. These calculations involve the photon parton distributions at $\hat{Q}_\gamma^2$ scales up to $\sim$ 1600 GeV^2 and fractional momenta down to $x_\gamma \sim 10^{-2}$. These parametrisations of the photon structure function differ mainly in their gluon content. The LAC1 set contains a larger contribution of gluons at low fractional momenta than the other sets. These differences are reflected in the predicted $d\sigma/d\eta^{jet}$ in the forward region. The prediction based on the LAC1 set increases for $\eta^{jet} > 1$ whereas the predictions based on the other sets remain relatively constant in this region (see Figure 2).

In Figure 2, the measured η^{jet} distribution integrated over $E_T^{jet} > 8$ GeV is compared to the Monte Carlo calculations using the sets of photon parton distributions mentioned above. The Monte Carlo calculation of $d\sigma/d\eta^{jet}$ for the direct processes alone, which does not involve the photon parton distributions, is also shown. It can be seen that the direct processes alone cannot describe the shape of the measured η^{jet}-spectrum for $\eta^{jet} > 0$ and that the resolved processes dominate throughout the η^{jet} range studied. In contrast, the shape and normalisation of $d\sigma/d\eta^{jet}$ of the data are well described in the region $-1 < \eta^{jet} < 1$ by the LO QCD

[3]The PYTHIA and POMPYT samples were added according to the cross sections given by the generators.

calculations of PYTHIA including resolved and direct processes and using LAC1, GRV-HO or ACFGP-HO(mc). The calculation using the set GS-HO can be brought into agreement with the data by an overall normalisation factor. This result does not support the discrepancy of $d\sigma/d\eta^{jet}$ with respect to LO QCD calculations observed by the H1 Collaboration [35].

In the region $1 < \eta^{jet} < 2$, the measured $d\sigma/d\eta^{jet}$ increases as η^{jet} increases. Although only the calculation using the LAC1 set gives a reasonable description of this rise, it cannot be concluded that the rise is due to the abundance of low x_γ gluons in the photon. As was observed in the jet profiles (see section 5), there is a significant excess of transverse-energy density in the data with respect to the Monte Carlo expectations for jets in the region $1 < \eta^{jet} < 2$. This excess is located outside of the jet in the forward direction, i.e. $\Delta\eta > 1$. The origin of this extra transverse energy is unclear, but one consequence might be that the transverse energy of the very forward jets is enhanced, and these jets, which otherwise would have not satisfied $E_T^{jet} > 8$ GeV, contribute to the cross section.

The behaviour of the measured $d\sigma/d\eta^{jet}$ as the E_T^{jet} threshold increases ($E_T^{jet} > 8$, 11 and 17 GeV) is shown in Figure 3. The increase of the measured $d\sigma/d\eta^{jet}$ in the very forward region observed for $E_T^{jet} > 8$ GeV is not present for higher E_T^{jet} thresholds. The Monte Carlo calculations including both resolved and direct processes and using any of the sets of photon parton distributions discussed above describe well the shape and magnitude of the measurements for the two highest E_T^{jet} thresholds over the entire η^{jet} range (only the calculations done with LAC1 or GRV-HO are shown in Figure 3). Thus, the discrepancies between the measurements and the LO QCD predictions are restricted to low E_T^{jet}, very forward jets. In order to understand the agreement at higher E_T^{jet} values, the jet profiles for the same E_T^{jet} thresholds have been studied (not shown). The excess of transverse energy density at $\Delta\eta > 1$ observed in the data with respect to the Monte Carlo expectations decreases as E_T^{jet} increases, but it is still present for the very forward jets. In addition, the relative importance of the possible extra contribution gets smaller as higher E_T^{jet} values are considered. As a result the effects on the cross section become less important. It is yet to be seen whether higher order QCD calculations in our kinematic regime will account for the discrepancies in the very forward, low E_T^{jet} region.

The comparison of the measured cross section for $E_T^{jet} > 17$ GeV to the Monte Carlo calculation of direct processes alone (see Figure 3) shows that even at these E_T^{jet} values the direct processes cannot describe the shape of the measured distribution and that the resolved processes still give the larger contribution to jet production. This result together with the successful comparisons between the measured $d\sigma/d\eta^{jet}$ for the two highest E_T^{jet} thresholds and the Monte Carlo calculations including resolved and direct processes show that LO QCD gives reasonable descriptions in this new kinematic regime of the structure of the photon.

In Figure 4, the measured cross sections, $d\sigma/dE_T^{jet}$, integrated over two η^{jet} ranges ($-1 < \eta^{jet} < 2$ and $-1 < \eta^{jet} < 1$) are compared to the Monte Carlo calculations. The contributions from direct processes alone cannot reproduce the shapes of the data, although they become increasingly important as E_T^{jet} increases. In contrast, the predictions including both resolved and direct processes give a good description of the measured cross sections. For the range $-1 < \eta^{jet} < 2$ the predictions using any of the sets of photon parton distributions considered describe the shape and normalisation of the measurements in the region $E_T^{jet} > 11$ GeV. The agreement between the predictions in this region is due to the fact that at these high E_T^{jet} values the calculations involve the photon parton distributions at high x_γ values, where existing measurements combined with the standard evolution equations impose tight constraints. At the lowest E_T^{jet} point, the predictions using GS-HO or ACFGP-HO(mc) fall below the data whereas LAC1 or GRV-HO agree with the data. However, the caveat related to the jet profiles

(see above) prevents us from drawing a firm conclusion concerning this lowest E_T^{jet} data point. The reason is that the discrepancies observed at this E_T^{jet} point are related to those seen in the measured $d\sigma/d\eta^{jet}$ for $E_T^{jet} > 8$ GeV at $\eta^{jet} > 1$. Figure 4 shows that they are not present at higher E_T^{jet} values, as was also discussed in connection with Figure 3. This can also be seen in the comparison of the measured $d\sigma/dE_T^{jet}$ integrated over $-1 < \eta^{jet} < 1$ to the Monte Carlo calculations. The agreement between the first data point and the predictions is better when the range $-1 < \eta^{jet} < 1$ is considered. These results extend the agreement with LO QCD calculations of $d\sigma/dE_T^{jet}$ reported in [14] to the two η^{jet} ranges and high E_T^{jet} values, $E_T^{jet} = 41$ GeV, measured here.

7 Summary and conclusions

Measurements of the differential cross sections for inclusive jet photoproduction in ep collisions at $\sqrt{s_{ep}} = 296$ GeV using the data collected by ZEUS in 1993 are presented. The ep jet cross sections, $d\sigma/d\eta^{jet}$ and $d\sigma/dE_T^{jet}$, refer to jets at the hadron level with a cone radius of one unit in $\eta - \phi$ space. These cross sections are given in the kinematic region defined by $Q^2 \leq 4$ GeV^2 and $0.2 < y < 0.85$. The cross section $d\sigma/d\eta^{jet}$ has been measured in the η^{jet} range between -1 and 2 integrated over E_T^{jet} from various thresholds ($E_T^{jet} > 8$, 11 and 17 GeV). The cross section $d\sigma/dE_T^{jet}$ has been measured in the E_T^{jet} range between 8 GeV and 41 GeV integrated over two η^{jet} ranges ($-1 < \eta^{jet} < 2$ and $-1 < \eta^{jet} < 1$). The η^{jet} range studied in the ep laboratory frame corresponds roughly to $-3 < \eta^{jet}(\gamma p \text{ CMS}) < 0$. These measurements probe a new kinematic regime of the partonic structure of the photon, which involves scales up to $(E_T^{jet})^2 \sim 300$ GeV^2 and fractional momenta down to $x_\gamma \sim 10^{-2}$. These cross sections could be directly compared to higher order QCD calculations, where the theoretical framework is well understood [6], but no results are currently available for our range of kinematic variables.

Leading logarithm parton shower Monte Carlo calculations using the predictions of currently available parametrisations of the photon parton distributions are compared to the measured jet cross sections. It is shown that contributions from the resolved processes are essential in describing the η^{jet}-spectrum for the different E_T^{jet} thresholds studied. For the lowest threshold ($E_T^{jet} > 8$ GeV) the data show an increase in the region $1 < \eta^{jet} < 2$ which is not reproduced by some of the calculations. For higher thresholds the calculations describe well the measured cross sections in the entire η^{jet} range. The measured E_T^{jet} cross sections exhibit the expected behaviour given by LO QCD up to the highest E_T^{jet} values studied. Except for the region of very forward, low E_T^{jet} jets, these measurements are fully consistent with LO QCD in this new kinematic regime of the structure of the photon.

Acknowledgements

We thank the DESY Directorate for their strong support and encouragement. The remarkable achievements of the HERA machine group were essential for the successful completion of this work and are greatly appreciated.

References

[1] J.F. Owens, Phys. Rev. D21 (1980) 54.

[2] W.J. Stirling and Z. Kunszt in Proceedings of HERA Workshop (1987) 331; M. Drees and F. Halzen, Phys. Rev. Lett. 61 (1988) 275; M. Drees and R.M. Godbole, Phys. Rev. D39 (1989) 169.

[3] H1 Collab., T. Ahmed et al., Phys. Lett. B297 (1992) 205.

[4] ZEUS Collab., M. Derrick et al., Phys. Lett. B297 (1992) 404.

[5] ZEUS Collab., M. Derrick et al., Phys. Lett. B322 (1994) 287.

[6] G. Kramer and S.G. Salesch in Proc. of the Workshop on Physics at HERA, DESY (1991) 649 and in DESY preprint, DESY-93-10; L.E. Gordon and J.K. Storrow, Phys. Lett. B291 (1992) 320; D. Bödeker, Phys. Lett. B292 (1992) 164; J.R. Forshaw and R.G. Roberts, Phys. Lett. B319 (1993) 539; M. Greco and A. Vicini, Nucl. Phys. B415 (1994) 386; D. Bödeker, G. Kramer and S.G. Salesch, DESY preprint, DESY-94-042.

[7] For a recent review see: H. Abramowicz et al., Int. Jour. of Mod. Phys. A8 (1993) 1005.

[8] M.Drees and K.Grassie, Z. Phys. C28 (1985) 451.

[9] H. Abramowicz, K. Charchuła and A. Levy, Phys. Lett. B269 (1991) 458.

[10] M. Glück, E. Reya and A. Vogt, Phys. Rev. D46 (1992) 1973.

[11] L.E. Gordon and J.K. Storrow, Z. Phys. C56 (1992) 307.

[12] P. Aurenche et al., Z. Phys. C56 (1992) 589.

[13] TOPAZ Collab., H. Hayashii et al., Phys. Lett. B314 (1993) 149; AMY Collab., B.J. Kim et al., Phys. Lett. B325 (1994) 248.

[14] H1 Collab., I. Abt et al., Phys. Lett. B314 (1993) 436.

[15] The ZEUS Detector, Status Report (1993), DESY 1993.

[16] ZEUS Collab., M. Derrick et al., Phys. Lett. B332 (1994) 228.

[17] A. Andresen et al., Nucl. Inst. Meth. A309 (1991) 101; A. Caldwell et al., Nucl. Inst. Meth. A321 (1992) 356; A. Bernstein et al., Nucl. Inst. and Meth. A336 (1993) 23.

[18] J. Andruszków et al., DESY 92-066 (1992).

[19] Method proposed by F. Jacquet and A. Blondel in Proc. of the Study for an *ep* Facility for Europe, U. Amaldi et al., DESY 79/48 (1979) 377.

[20] G. D'Agostini and D. Monaldi, Z. Phys. C48 (1990) 467; K.J. Abraham et al., Proc. of ECFA Workshop on LHC, Aachen (1990) 899; R. van Woudenberg et al., Proc. of the Workshop on Physics at HERA, DESY (1991) 739.

[21] ZEUS Collab., M. Derrick et al., Phys. Lett. B293 (1992) 465.

[22] H.-U. Bengtsson and T. Sjöstrand, Comp. Phys. Comm. 46 (1987) 43 and T. Sjöstrand, CERN-TH.6488/92.

[23] G. Marchesini et al., Comp. Phys. Comm. 67 (1992) 465.

[24] R. Kleiss et al., in 'Z Physics at LEP 1', eds. G. Altarelli, R. Kleiss and C. Verzegnassi, CERN-89-08, Vol. 3, p.1.

[25] A.D. Martin, W.J. Stirling and R.G. Roberts, Phys. Rev. D47 (1993) 867.

[26] B. Andersson et al., Phys. Rep. 97 (1983) 31.

[27] T. Sjöstrand, Comp. Phys. Comm. 39 (1986) 347; T. Sjöstrand and M. Bengtsson, Comp. Phys. Comm. 43 (1987) 367.

[28] G. Ingelman and P.E. Schlein, Phys. Lett. 152B (1985) 256; E.L. Berger et al., Nucl. Phys. B286 (1987) 704; K.H. Streng, Proc. of HERA Workshop, DESY (1987) 365; A. Donnachie and P.V. Landshoff, Nucl. Phys. B303 (1988) 634, Phys. Lett. B285 (1992) 172; J.C. Collins et al., Phys. Lett. B307 (1993) 161.

[29] ZEUS Collab., presented by J. Whitmore, 'Observation of Hard Scattering in Photoproduction Events with a Large Rapidity Gap at HERA', to appear in the Proc. of the International Workshop on Deep Inelastic Scattering and Related Subjects, edited by A. Levy, Eilat, Israel, February 1994; H1 Collab., presented by T. Greenshaw at the 29th Rencontres de Moriond (Méribel les Allues, France, March 1994) and preprint DESY-94-112.

[30] P. Bruni and G. Ingelman, Proc. of the International Europhysics Conference, edited by J. Carr and M. Perrotet, Marseille, France, July 1993 (Ed. Frontieres, Gif-sur-Yvette, 1994, p. 595).

[31] UA1 Collab., G. Arnison et al., Phys. Lett. 123B (1983) 115.

[32] J. Huth et al., Proc. of the 1990 DPF Summer Study on High Energy Physics, Snowmass, Colorado, edited by E.L. Berger (World Scientific, Singapore,1992) p. 134.

[33] K. Desch, Ph.D. Thesis, Physikalisches Institut der Universität Bonn (1994).

[34] C. Glasman, Ph.D. Thesis, Weizmann Institute of Science (1994).

[35] See [14]; however, an update of these measurements by the H1 Collaboration has been recently presented: H. Hufnagel, Proc. of the International Conference on High Energy Physics, Glasgow, Scotland, July (1994).

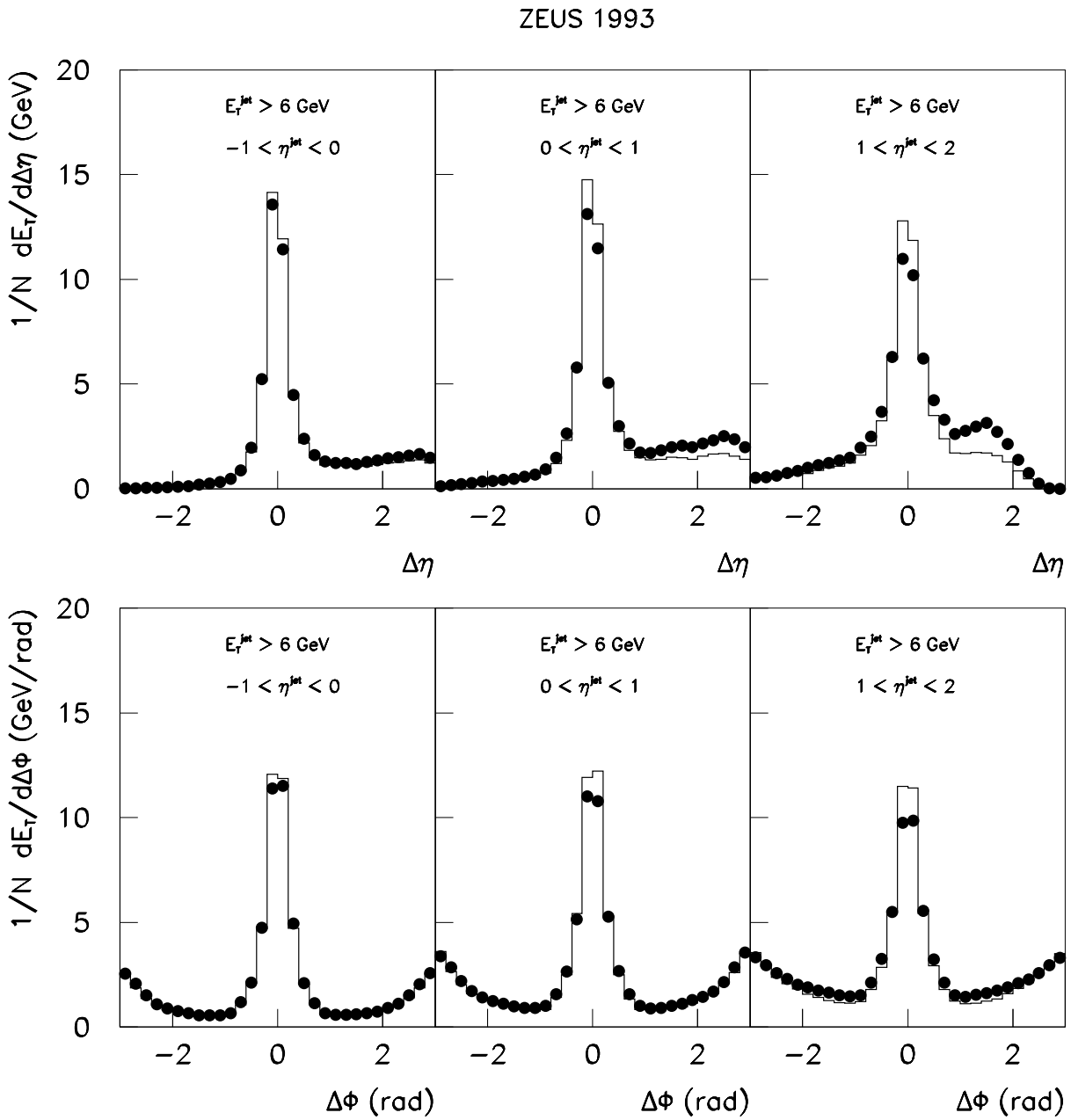

Figure 1: Transverse energy profiles as functions of the distance from the jet axes, $\Delta\eta$ (integrated over $|\Delta\phi| < \pi/2$; top row) and $\Delta\phi$ (integrated over $|\Delta\eta| < 1$; bottom row), for jets with $E_{T,cal}^{jet} > 6$ GeV and $-1 < \eta_{cal}^{jet} < 2$ in the data (black dots; the statistical errors are smaller than the size of the symbols) and PYTHIA Monte Carlo samples including both resolved and direct processes (histogram).

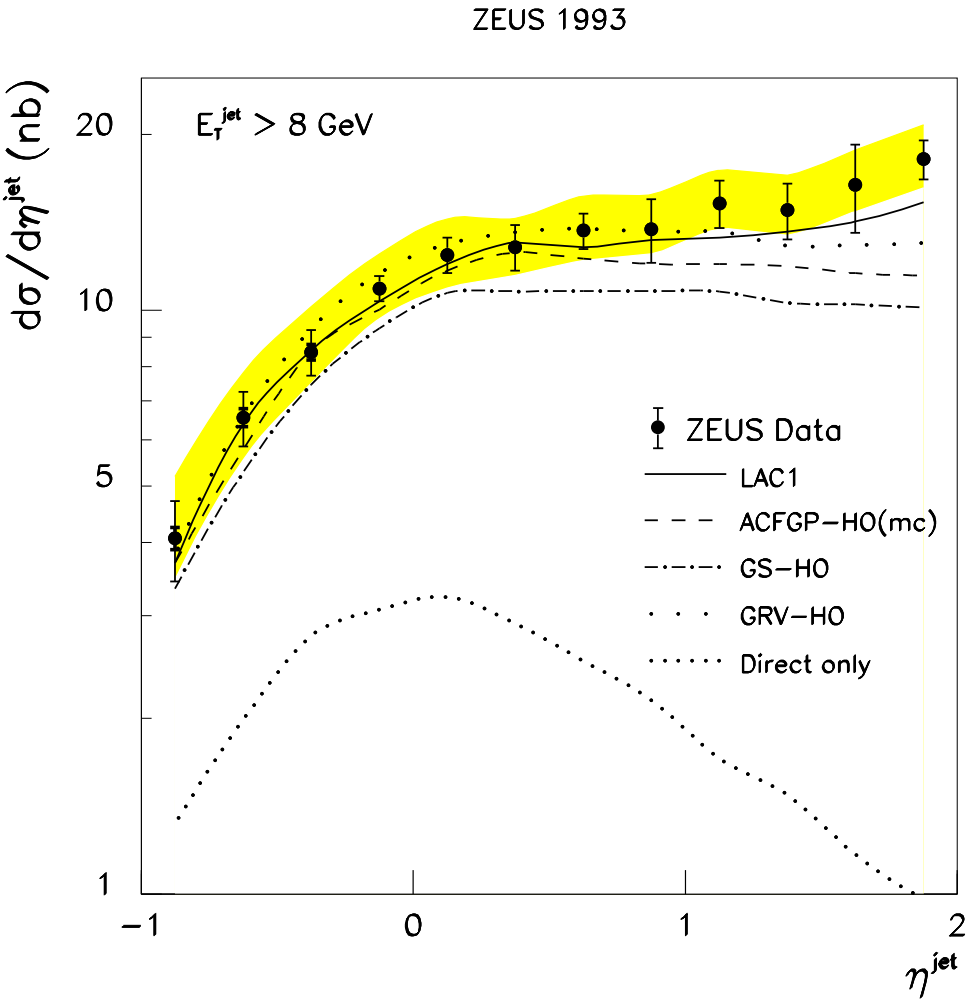

Figure 2: Measured differential ep cross section $d\sigma/d\eta^{jet}$ for inclusive jet production integrated over $E_T^{jet} > 8$ GeV in the kinematic region defined by $Q^2 \leq 4$ GeV^2 and $0.2 < y < 0.85$ (black dots). The thick error bars represent the statistical errors of the data, and the thin error bars show the statistical and systematic errors —not associated with the energy scale of the jets— added in quadrature. The shaded band displays the uncertainty due to the energy scale of the jets. For comparison, PYTHIA calculations including direct (close-dotted line) and resolved plus direct processes for various parametrisations of the photon parton distributions (LAC1, solid line; GRV-HO, wide-dotted line; GS-HO, dot-dashed line; ACFGP-HO(mc), dashed line) are also shown. In all cases, the MRSD$_-$ proton parton distributions have been used.

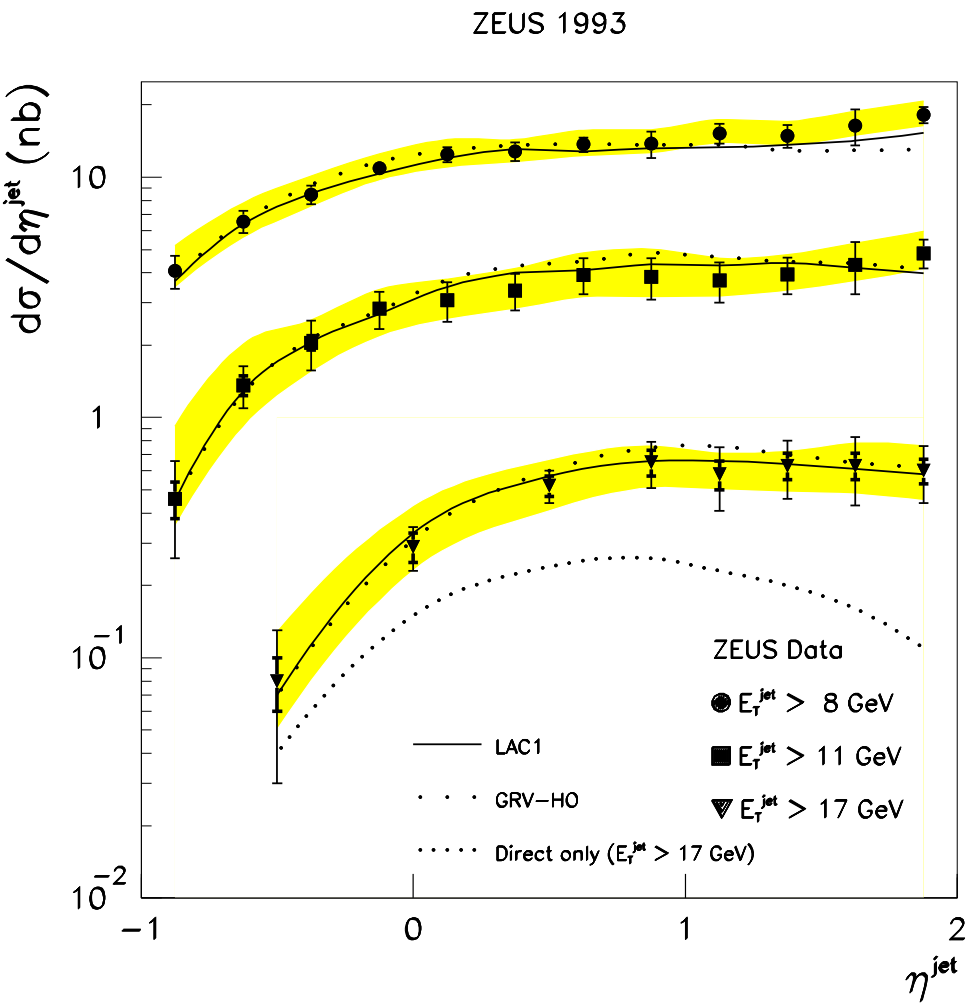

Figure 3: Measured differential ep cross section $d\sigma/d\eta^{jet}$ for inclusive jet production integrated over E_T^{jet} from three different thresholds ($E_T^{jet} > 8$, 11 and 17 GeV) in the kinematic region defined by $Q^2 \leq 4$ GeV^2 and $0.2 < y < 0.85$. The thick error bars represent the statistical errors of the data, and the thin error bars show the statistical and systematic errors –not associated with the energy scale of the jets– added in quadrature. The shaded bands indicate the uncertainty due to the energy scale of the jets. For comparison, PYTHIA calculations including resolved plus direct processes and using the LAC1 (solid lines) or GRV-HO (wide-dotted lines) set of photon parton parametrisations are also displayed. The PYTHIA calculation for $E_T^{jet} > 17$ GeV including only direct processes (close-dotted line) is also shown. In all cases, the MRSD$_-$ set of proton parton distributions has been used.

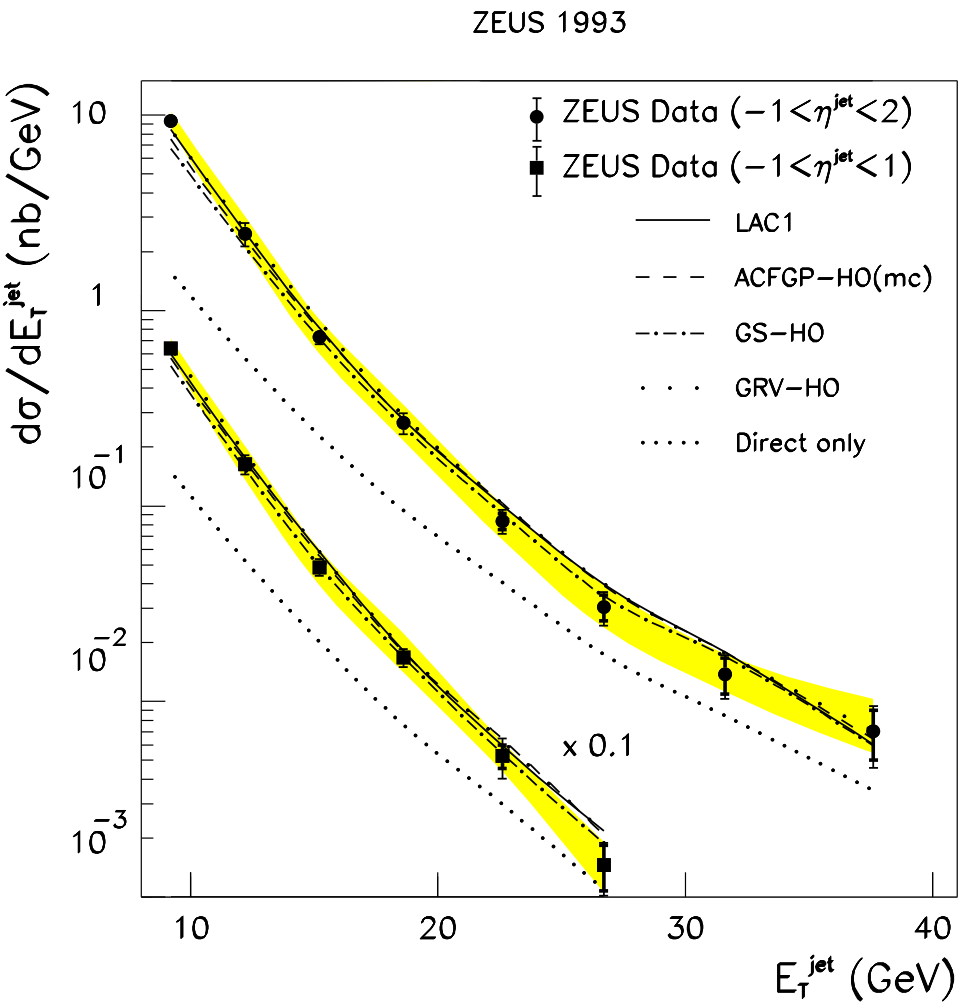

Figure 4: Measured differential ep cross section $d\sigma/dE_T^{jet}$ for inclusive jet production integrated over two η^{jet} ranges ($-1 < \eta^{jet} < 2$ and $-1 < \eta^{jet} < 1$; for the latter, both measurements and Monte Carlo calculations have been multiplied by 0.1) in the kinematic region defined by $Q^2 \leq 4$ GeV^2 and $0.2 < y < 0.85$ (solid points). The thick error bars represent the statistical errors of the data, and the thin error bars show the statistical and systematic errors −not associated with the energy scale of the jets− added in quadrature. The shaded bands indicate the uncertainty due to the energy scale of the jets. For comparison, PYTHIA calculations including direct (close-dotted lines) and resolved plus direct processes for various parametrisations of the photon parton distributions (LAC1, solid line; GRV-HO, wide-dotted line; GS-HO, dot-dashed line; ACFGP-HO(mc), dashed line) are also shown. In all cases, the MRSD$_-$ proton parton distributions have been used.